

Crotoxin suppresses the tumorigenic properties and enhances the antitumor activity of Iressa® (gefinitib) in human lung adenocarcinoma SPCA-1 cells

JUNHUA WANG¹, XIUGUANG QIN², ZHIQIANG ZHANG³, MEILING CHEN⁴, YING WANG⁴ and BAOQIN GAO⁵

Departments of ¹Cardiothoracic Surgery, ²Thoracic Surgery, ³Respiratory Medicine, ⁴Oncology and ⁵Operating Room, The First Hospital Affiliated to the Xinxiang Medical College, Xinxiang, Henan 453100, P.R. China

Received January 10, 2014; Accepted July 4, 2014

DOI: 10.3892/mmr.2014.2620

Abstract. Crotoxin (CrTX) is a neurotoxin isolated from the venom of the South American rattlesnake. Previous studies demonstrated that CrTX was able to inhibit the activity of the growth factor receptor tyrosine kinase and that CrTX possesses potent antitumor activity when combined with Iressa, an epidermal growth factor receptor inhibitor. The aim of the present study was to determine the antitumor effect of CrTX and the combination of CrTX with Iressa in lung adenocarcinoma SPCA-1 cells. The results demonstrated that CrTX inhibited the cellular growth of SPCA-1 cells via G1 arrest and induction of apoptosis. In addition, the c-Jun N-terminal kinase pathway was important in CrTX-induced apoptosis in SPCA-1 cells. Notably, CrTX was able to significantly enhance the cytotoxic effects of Iressa in SPCA-1 cells. The *in vivo* antitumor assay demonstrated that treatment with either CrTX or Iressa significantly inhibited tumor growth, while the combination of CrTX and Iressa demonstrated the most significant antitumor activity, which was reflected by tumor weight and angiogenesis, presented as microvascular density. Therefore, the present study suggested that CrTX is a potential anti-lung cancer agent and sensitizer of Iressa.

Introduction

Lung cancer is the most common type of malignant cancer with the highest mortality rate in humans (1). The prognosis of lung cancer is extremely poor and only a small percentage of patients are eligible for potential curative treatments, including resection, transplantation or local ablation. According to the US Centers

for Disease Control and Prevention, the overall 5-year survival rate of lung cancer is only 8-14% following diagnosis (2). One type of lung cancer, lung adenocarcinoma, is a non-small cell lung cancer (NSCLC) that accounts for ~40% of cases of lung cancer (3). In the past few decades, its incidence has increased in numerous countries, where it has become the most prevalent subtype of lung cancer (4). Chemotherapy has been commonly used to extend the lifespan of patients with lung adenocarcinoma. However, intense chemotherapy often causes drug resistance and severe side effects. Accordingly, novel therapeutic approaches, including molecular targeted therapies, are urgently required in order to efficiently treat lung adenocarcinoma.

Crotoxin (CrTX), a cytotoxic phospholipase A2 (PLA2), is isolated from the venom of the South American rattlesnake, *Crotalus durissus terrificus* (5). It is a complex composed of two non-identical subunits, subunit A and B. Subunit B possesses PLA2 activity and contributes to the cytotoxicity of CrTX (6). The biological activities of CrTX include neurotoxicity, immunomodulatory, anti-inflammatory, antimicrobial and analgesic actions. Notably, CrTX has demonstrated cytotoxic effects in a variety of human tumor cell lines *in vitro*, including K562 leukemia cells, MCF-7 breast cancer cells as well as A549 and SK-MES-1 lung cancer cells (7,8). The mechanism underlying the cytotoxic effects of CrTX in A549 and SK-MES-1 lung cancer cells includes cellular proliferation inhibition and apoptosis, associated with activation of caspase-3, c-Jun N-terminal kinase (JNK), p53 and p38. In addition, CrTX demonstrated synergistic antitumor effects in lung cancer when combined with Iressa, an epidermal growth factor receptor (EGFR) inhibitor currently widely used in lung cancer therapy (7,9).

The present study investigated whether CrTX was able to suppress the tumorigenic properties and enhance the antitumor activity of Iressa in human lung adenocarcinoma SPCA-1 cells.

Materials and methods

Cell culture. Human lung adenocarcinoma SPCA-1 cells were purchased from the Shanghai Institute of Cell Biology, Chinese Academy of Sciences (Shanghai, China). The cells were grown in high glucose Dulbecco's modified Eagle's medium (Gibco-BRL, Carlsbad, CA, USA) with 10% heat-inactivated fetal bovine serum (HyClone Laboratories, Inc., Logan,

Correspondence to: Dr Junhua Wang, Department of Cardiothoracic Surgery, The First Hospital Affiliated to the Xinxiang Medical College, 88 Jiankang Road, Weihui, Henan 453100, P.R. China
E-mail: doctorjh1981@163.com

Key words: crotoxin, Iressa, human lung adenocarcinoma, SPCA-1 cells

UT, USA) in a 5% CO₂ atmosphere at 37°C and routinely subcultured every 3 days. The present study was performed according to the Guidelines of the Medical Ethical Committee of Xinxiang Medical College (Xinxiang, China)

Drug treatment. CrTX was purchased from Celtic Biotech Ltd. (Dublin, Ireland). The CrTX was identified, as previously described (10). Iressa (gefitinib) was obtained from AstraZeneca (London, UK). The cells in mid-log phase were used in all the experiments. To investigate the dose and time response of SPCA-1 cells to CrTX, the SPCA-1 cells were plated onto 96-well microplates at a density of 1x10⁴ cells per well and cultured for 16 h. Following this, a series of concentrations of CrTX (12.5, 25, 50 and 100 µg/ml), Iressa (1.25, 2.5, 5 and 10 µmol/l), Iressa (2.5 µmol/l) combined with CrTX (12.5, 25, 50 and 100 µg/ml) or CrTX (25 µg/ml) combined with Iressa (1.25, 2.5, 5 and 10 µmol/l) were added to the cells. At different time periods, cellular responses, including cell viability and colony formation efficiency were evaluated.

Cell viability assays and cell colony formation. Cell viability was assessed using an MTT assay (Roche Diagnostics, Mannheim, Germany) according to the manufacturer's instructions 24 and 48 h after drug treatment as previously described. The colony formation assay was performed, as previously described (11), with slight modification. In brief, the cells were seeded onto 10 cm dishes (1,000 cells/dish). After 24 h, when the cells adhered to the plate, the medium was removed and CrTX (12.5, 25, 50 and 100 µg/ml), Iressa (1.25, 2.5, 5 and 10 µmol/l), Iressa (2.5 µmol/l) combined with CrTX (12.5, 25, 50 and 100 µg/ml) or CrTX (25 µg/ml) combined with Iressa (1.25, 2.5, 5 and 10 µmol/l) was applied to the medium to treat the cells for 72 h. Subsequently, the medium was changed to a fresh medium and the cells were incubated for 14 days in an atmosphere containing 5% CO₂ at 37°C. The colonies were fixed with cold methanol (Sigma-Aldrich, St Louis, MO, USA) for 10 min, stained with crystal violet (Sigma-Aldrich) and counted by eye.

Cell cycle and apoptosis assays. To perform the cell cycle assays, the cells were washed with cold phosphate-buffered saline (PBS; HyClone Laboratories, Inc.) and fixed with 70% cold alcohol overnight. The fixed cells were then collected, washed in PBS and stained with propidium iodide (PI; Sigma-Aldrich-Aldrich) in the presence of RNAase (Sigma-Aldrich). The cell cycle was examined by flow cytometry (Becton-Dickinson, San Jose, CA, USA) using ModFit LT™ for Windows version 3.2 software. To evaluate cell apoptosis, an Annexin-V fluorescent fluorescein isothiocyanate (FITC) Apoptosis kit (Cell Signaling Technology, Inc., Boston, MA, USA) was used. Briefly, cells were harvested, washed with cold PBS and resuspended with the 10X Annexin V Binding Buffer (Cell Signaling Technology, Inc.), followed by incubation with Annexin-V FITC and PI buffers (Cell Signaling Technology, Inc.) in the dark at 4°C for 15 min. Cell apoptosis was examined using flow cytometry.

Western blot analysis. Western blot analysis was performed as described previously (12). In brief, collected cells were

sonicated on ice in a radioimmunoprecipitation assay buffer. The cells were then centrifuged at 12,000 x g at 4°C for 20 min and the supernatant was preserved at -80°C for further analysis. The protein concentration was measured using a bicinchoninic acid protein assay kit (Pierce Biotechnology, Inc., Rockford, IL, USA). Extracted protein (40 µg) was subjected to SDS-polyacrylamide gel electrophoresis and transferred onto polyvinylidene fluoride membranes. The mouse monoclonal anti-human p-JNK antibody (final dilution 1:1,000; Cell Signaling Technology, Inc.) was used as a primary antibody and the horseradish peroxidase-labeled goat monoclonal anti-mouse IgG (final dilution 1:2,000; Cell Signaling Technology, Inc.) was used as a secondary antibody. The β-actin antibody (final dilution 1:5,000; Sigma-Aldrich) was used as an internal control. The bands were detected using an Enhanced Chemiluminescence kit (GE Healthcare, Pittsburgh, PA, USA) and visualized using the ChemiDoc XRS system (Bio-Rad, Hercules, CA, USA).

In vivo antitumor assays. All Balb/c nude mice were maintained in filter-topped cages on an autoclaved normal chow diet in a specific pathogen free animal room. They were acclimated for 1 week prior to being used in the investigation. All procedures were performed in accordance with the Guidelines of the Chinese Association for Laboratory Animal Science. For *in vivo* antitumor assays, Balb/c nude mice (5-6 weeks; male; ~20 g) were inoculated subcutaneously on the flank with 1x10⁷ SPCA-1 cells suspended in 0.1 ml PBS. At 11 days after inoculation, the mice were treated with a negative control (PBS), CrTX (10 µg/kg intraperitoneally, twice a week), Iressa (100 mg/kg/day intragastrically, daily) and CrTX combined with Iressa (CrTX 10 µg/kg intraperitoneally, twice a week, Iressa 100 mg/kg/day intragastrically, daily). Therapy was provided for 30 days. Mice were sacrificed at the end of the 30 day treatment and the tumors were excised and weighed.

Immunofluorescence assays. The cells were incubated with the primary p-JNK antibody (final dilution 1:1,000; Cell Signaling Technology, Inc.) at 4°C overnight, followed by methanol fixation and 1% bovine serum albumin dissolved in 0.1% Triton X-100 (Sigma-Aldrich). FITC-labeled goat monoclonal anti-mouse IgG (final dilution 1:5,000; Sigma-Aldrich) was used as a secondary antibody to detect the primary antibody bound to the cells. Finally, the stained cells were observed using a laser confocal microscope (Leica TCS SP5; Leica Microsystems, Wetzlar, Germany).

Immunohistochemistry assays. The expression of CD34 in the tumor xenografts was detected using immunohistochemistry assays (13). Briefly, the paraffin sections of the excised tumors were stained with mouse monoclonal anti-human CD34 antibody (Boshide Biotechnology Co., Wuhan, China). Subsequently, FITC-labeled goat anti-mouse IgG (final dilution 1:5,000; Sigma-Aldrich, St. Louis, MO, USA) was used as a secondary antibody to detect the primary antibody bound to the cells. Under a fluorescence microscope (Nikon Eclipse TE 300; Nikon Corporation, Tokyo, Japan), CD34-positive cells were detected and the microvascular density (MVD) was counted using Weidner's method (14).

Transmission electron microscopy (TEM). The tumor xenografts were fixed in ice-cold glutaraldehyde (2.5%; Sigma-Aldrich) in 0.1 mol/l PBS and maintained at 4°C. Following this, the cells were post fixed in the same buffer with 1% osmium tetroxide (Sigma-Aldrich) and dehydrated in graded alcohols. The cells were then embedded in Epon 812 (Sigma-Aldrich), sectioned using an ultramicrotome (RMC PowerTome-PC; Boeckeler Instruments, Inc., Tucson, AZ, USA), stained with uranyl acetate and lead citrate, followed by examination using TEM Philips Tecnai 10; Philips, Eindhoven, Netherlands).

Statistical analysis. Data in the present study were analyzed using the statistics package SPSS 13.0 (SPSS, Inc., Chicago, IL, USA). Data are expressed as the mean \pm standard error of the mean. Statistical significance between three or more groups was assessed using one-way analysis of variance followed by Dunnett's t-test. $P < 0.05$ was considered to indicate a statistically significant difference.

Results

CrTX combined with Iressa inhibits the tumorigenic properties of SPCA-1 cells. To investigate the antitumor effect of CrTX in SPCA-1 cells, the cells were exposed to various doses of CrTX or Iressa for different time periods. The results demonstrated that CrTX and Iressa inhibited cell viability in a time- and dose-dependent manner (Fig. 1A and B). When CrTX and Iressa were combined, the inhibitory rate was increased significantly compared with CrTX or Iressa alone (Fig. 1A and B). The enhanced inhibitory rate of the combination of CrTX and Iressa was also observed in the cell colony formation assay (Fig. 1C and D). The Q score (cell viability assays: 0.87-1.06; cell colony formation assays: 0.88-1.11) suggested that there was an additive effect when CrTX was combined with Iressa *in vitro*. The Q score is a measure of confidence. These results demonstrated that CrTX combined with Iressa inhibited the tumorigenic properties of SPCA-1 cells.

CrTX induces G1 arrest and cell apoptosis in SPCA-1 cells. To further elucidate the antitumor mechanism of CrTX in SPCA-1 cells, cell cycle and cell apoptosis were examined. Following 24 h treatment, CrTX and Iressa significantly increased the percentage of cells in the G1 phase compared with the control group. The combination of CrTX and Iressa further increased the percentage of cells in the G1 phase (Fig. 2A; Table I).

Similarly, the apoptotic rates of SPCA-1 cells in the CrTX, Iressa and CrTX combined with Iressa treated groups were markedly increased compared with the control group (Fig. 2B and Table I). To determine the mechanism for apoptosis, SPCA-1 cells were treated with SP600125, a specific JNK inhibitor. Notably, following treatment with SP600125, the apoptotic rate in the CrTX group was significantly reduced (Fig. 2B and Table I). These results suggested that CrTX and Iressa inhibited the growth of SPCA-1 cells via G1 arrest and induction of apoptosis, and that JNK was important in CrTX-induced apoptosis in SPCA-1 cells.

CrTX activates the JNK pathway in SPCA-1 cells. To confirm whether CrTX-induced cell apoptosis was associated

Table I. CrTX induces G1 arrest and apoptosis in SPCA-1 cells.

Group	G1 phase (%)	Apoptosis (%)
Control	42.46 \pm 3.30	0.89 \pm 0.06
CrTX	52.42 \pm 1.14 ^a	15.8 \pm 1.20 ^a
Iressa	56.64 \pm 2.50 ^a	13.6 \pm 1.40 ^a
CrTX + Iressa	69.98 \pm 2.04 ^{a,b}	22.8 \pm 2.80 ^{a,b}
CrTX + SP600125	-	1.21 \pm 0.04 ^b

Data are expressed as the mean \pm standard error of the mean. ^a $P < 0.05$, vs. control; ^b $P < 0.05$, vs. CrTX or Iressa, $n = 6$. CrTX, crotoxin.

with activation of the JNK pathway, the expression level of phosphorylated JNK (p-JNK) was assessed by western blot analysis and immunofluorescence assays. Western blot analysis demonstrated that the level of p-JNK was upregulated following treatment with CrTX (Fig. 3A). In addition, immunofluorescence assays also confirmed the enhanced expression of p-JNK in SPCA-1 cells following treatment with CrTX, whereas SP600125 failed to change the level of CrTX-induced p-JNK expression (Fig. 3B). These results suggested that the JNK pathway is important in CrTX-induced apoptosis in SPCA-1 cells.

CrTX and Iressa suppress tumor growth by impairing the vascular basement membrane *in vivo*. In order to investigate the antitumor effect of CrTX and Iressa in SPCA-1 cells *in vivo*, a human SPCA-1 lung cancer model was established in nude mice. The results demonstrated that treatment with either CrTX or Iressa significantly inhibited the growth of tumors compared with the control. The combination of CrTX and Iressa revealed the most significant antitumor activity, as reflected by the tumor weight and angiogenesis (presented as MVD; Fig. 4A and B).

To determine the variation in the capillaries of tumor xenografts, the capillaries were observed using TEM. In the control group, the structure of the endothelial cells was normal and the development of the basal membrane was unabridged. However, TEM revealed expansive endoplasmic reticulum, swollen mitochondria and cracked microvascular basement membranes in the groups treated with CrTX or Iressa alone. In the combined treatment group, the alterations in the capillaries were the most evident, accompanied by narrow lumen and electron-dense material in the vascular endothelial cells (Fig. 4C). These results demonstrated that the antitumor mechanism of CrTX and Iressa *in vivo* involves anti-angiogenesis.

Discussion

CrTX, a snake toxin with intrinsic phospholipase activity, exists as a 24 kDa heterodimeric complex, subunit B possesses phospholipase activity, while subunit A is postulated to act as a chaperone (3,15). Although complex dissociation is essential for the anti-proliferative activity of CrTX, subunit A is indispensable for the selective binding of subunit B to cell surfaces (4,7). Several venoms deficient in intrinsic phospholipase activity also have an affinity for cellular membranes (16).

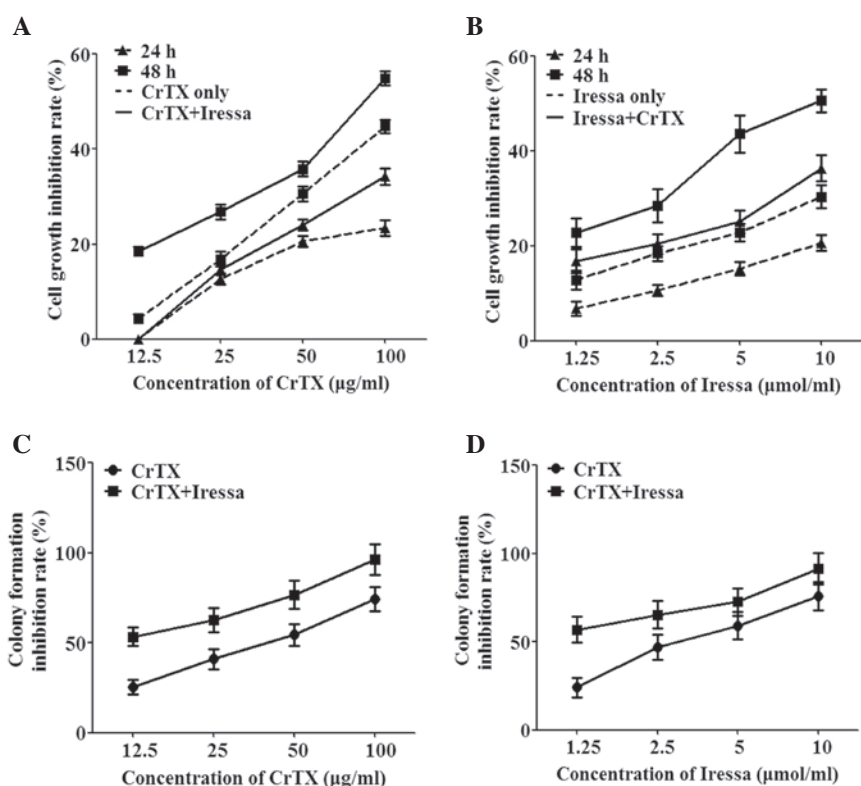


Figure 1. CrTX combined with Iressa inhibits the growth of SPCA-1 cells. (A and B) Effect of CrTX and/or Iressa on cell growth. The cell viability of SPCA-1 cells was measured using an MTT assay 24 and 48 h after drug treatment, as described in the Materials and methods. Cell viability was calculated using the following formula: $(A_E - A_B) / (A_C - A_B)$. A_E , A_C and A_B were defined as the absorbance of experimental samples, untreated samples and blank controls, respectively. (C and D) Effect of CrTX and/or Iressa on colony formation. Data are expressed as the mean \pm standard error of the mean ($n=3$). CrTX, crotoxin.

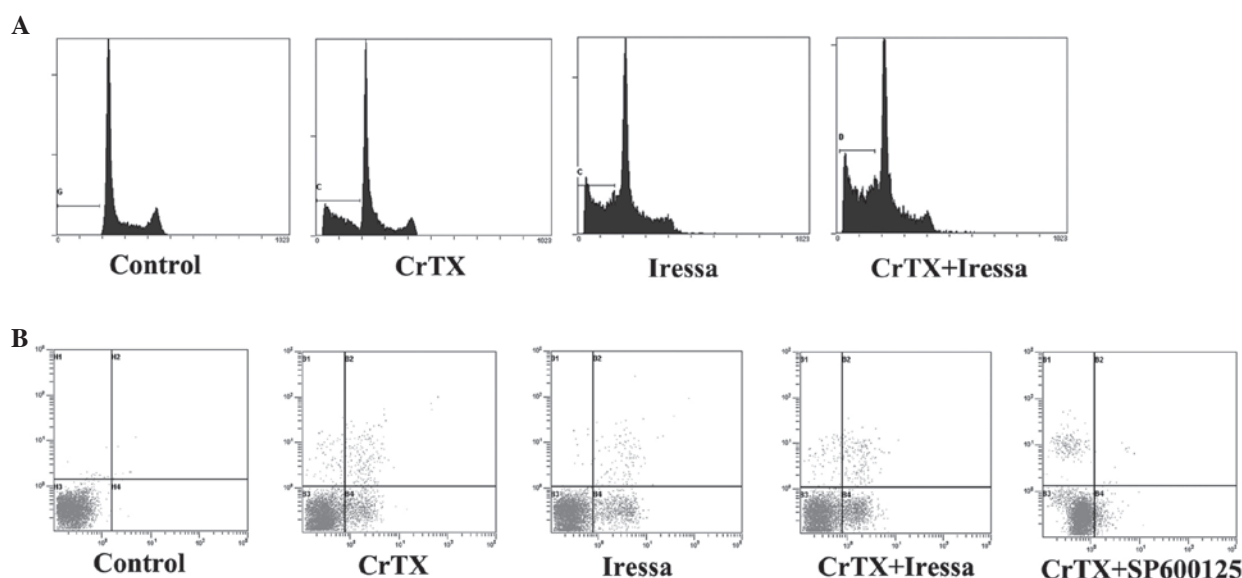


Figure 2. CrTX induces G1 arrest and cell apoptosis in SPCA-1 cells. (A) Cell cycle and (B) apoptosis were analyzed by flow cytometry following treatment with saline, CrTX (25 μ g/ml), Iressa (2.5 μ mol/l), CrTX (25 μ g/ml) combined with Iressa (2.5 μ mol/l) or CrTX (25 μ g/ml) + SP600125 (10 μ mol/l) for 24 h. Data are one representative of three independent experiments. CrTX, crotoxin.

The distinct cytotoxicity and affinity of venomous toxins may imply that venoms, including CrTX, can inhibit cell growth dependent on cell membrane integrity and activation of membrane receptor-dependent signaling pathways, such as the EGFR pathway.

Previous studies have reported the antitumor activity of CrTX against various types of tumor *in vitro* and *in vivo* (10,14,17,18). A previous study demonstrated that CrTX enhanced the antitumor activity of Iressa in SK-MES-1 human lung squamous carcinoma cells (12). Iressa is a tyrosine kinase

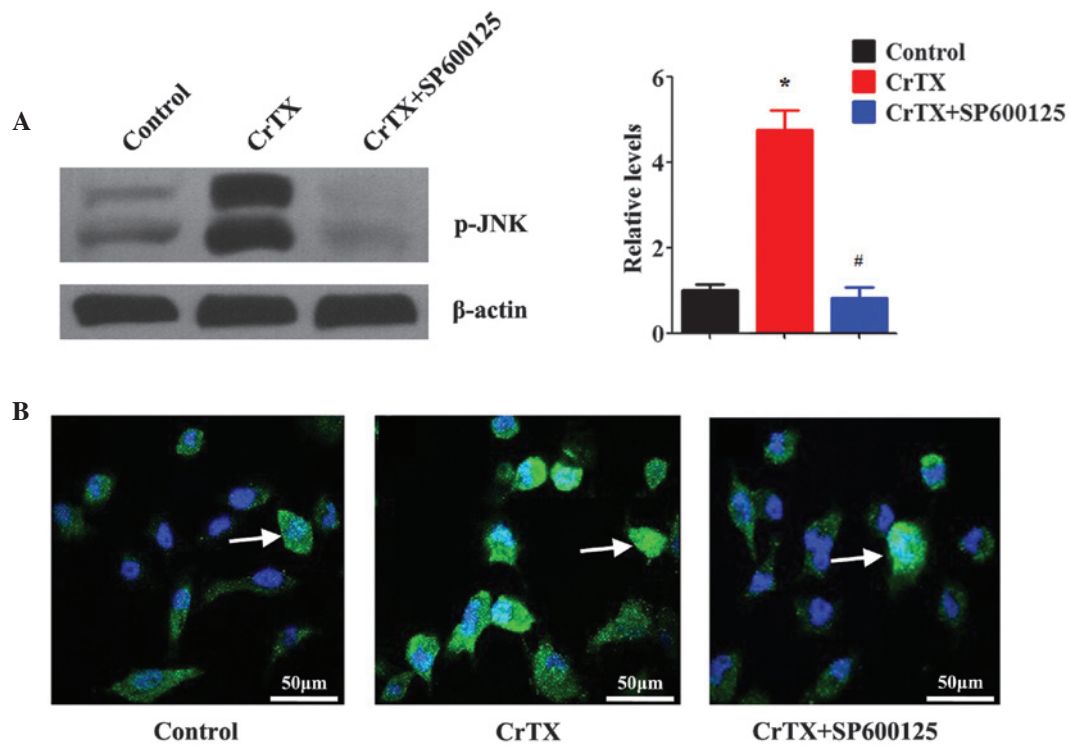


Figure 3. CrTX activates the JNK pathway in SPCA-1 cells. SPCA-1 cells were seeded onto a 6-well plate and treated with saline, CrTX (25 μ g/ml) or CrTX (25 μ g/ml) + SP600125 (10 μ mol/l) for 24 h. (A) Western blot analysis of p-JNK following treatment with β -actin as the loading control. Relative expression of p-JNK was calculated based on densitometric analysis of band intensities. (B) p-JNK was determined with immunofluorescence. White arrows indicate p-JNK expression. Data are one representative of three independent experiments and are expressed as the mean \pm standard error of the mean (n = 3). *P<0.05, vs. control; #P<0.05, vs. CrTX. CrTX, crotoxin; p-JNK, phosphorlated c-Jun N-terminal kinase.

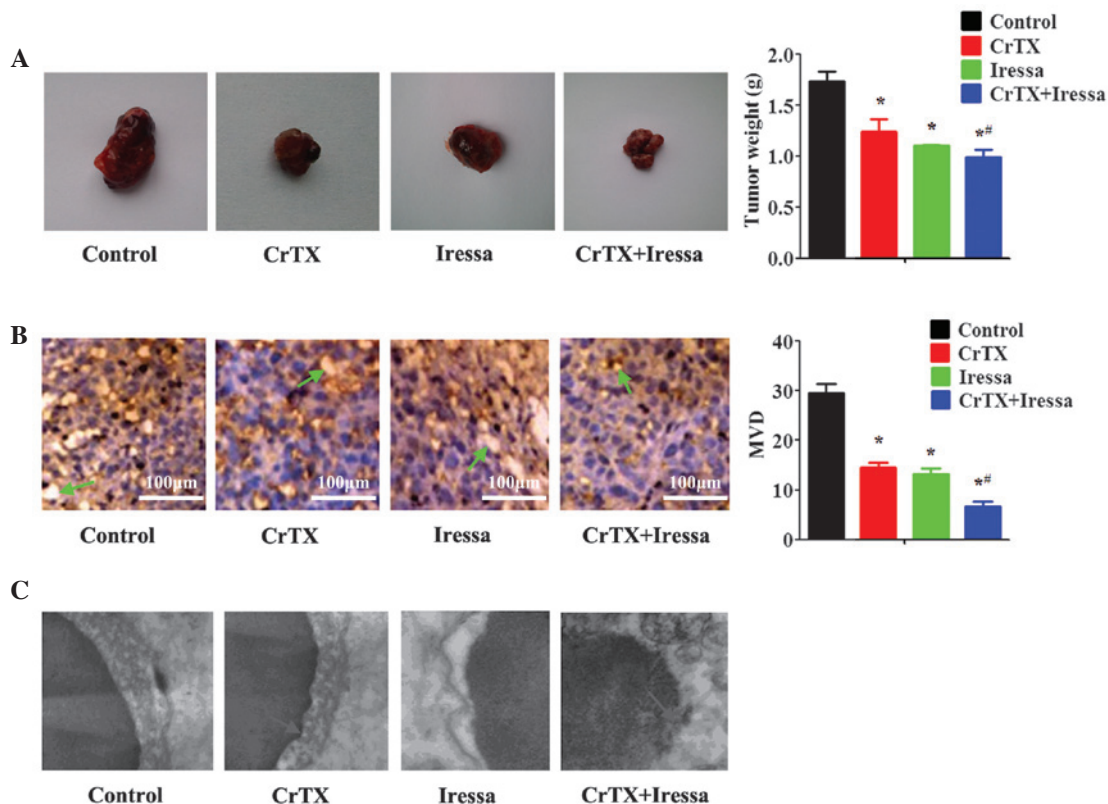


Figure 4. Antitumor assays *in vivo*. At 11 days after tumor inoculation, mice received various treatments for 30 days. The mice were euthanized after 30 days treatment. (A) Excised tumor weights. (B) CD34 staining by immunochemistry in excised tumors. The paraffin sections of the excised tumors were observed under a fluorescence microscope and MVD was counted using Weidner's method. Green arrows indicate CD34-positive cells. (C) Capillaries of the excised tumors were analyzed using transmission electron microscopy. Blue arrows indicate microvascular basal membrane abridgement. Data are expressed as the mean \pm standard error of the mean (n=3). *P<0.05, vs. control; #P<0.05, vs. CrTX or Iressa. MVD, microvascular density; CrTX, crotoxin.

inhibitor (TKI), which competes with adenosine triphosphate in binding to the intracellular domain of EGFR (19). It is widely used in the treatment of NSCLC. However, its efficacy is limited by either primary or acquired resistance to EGFR-TKI treatment following a median of ~10 months from the initiation of treatment (20). The present study confirmed that CrTX suppressed the tumorigenic properties in SPCA-1 cells and sensitized these cells to Iressa. These findings are consistent with a previous study that reported the enhanced antitumor effect of CrTX combined with Iressa in SK-MES-1 human lung squamous carcinoma cells, suggesting that CrTX may be a useful adjunctive therapy for lung cancer treatment (12).

The present study also suggested that CrTX may have antitumor activity in SPCA-1 cells through modulation of the EGFR signaling pathway. EGFR is a transmembrane protein belonging to the EGFR family of receptor tyrosine kinases. The activation of EGFR via ligand binding results in signaling through various pathways, resulting in cellular proliferation, survival, angiogenesis, invasion and metastasis (21). A previous study demonstrated that CrTX-induced cytotoxic effects are highly selective towards EGFR-overexpressing cell lines, suggesting that CrTX may have a high affinity for EGFR (15). Notably, the fact that CrTX promotes the phosphorylation of EGFR without any activation effect is somewhat unexpected, however, the mechanism remains to be elucidated. A plausible interpretation is that CrTX has a dual effect on the EGFR signaling pathway by targeting different sites.

A previous study also suggested that CrTX-induced apoptosis and cell cycle arrest in human lung squamous carcinoma SK-MES-1 cells are the main mechanisms underlying the CrTX-induced cytotoxic effects (12). The present study demonstrated that CrTX induced cell apoptosis via activation of the JNK pathway and G1 arrest in lung cancer SPCA-1 cells, suggesting an identical mechanism in different lung cancer cells. In addition, *in vivo* antitumor assays revealed that CrTX and Iressa induced a decrease in MVD concomitant with capillary structure damage, suggesting that the antitumor mechanism of CrTX and Iressa may include anti-angiogenesis.

Taken together, the results of the present study provide insights into the antitumor effect of CrTX in lung cancer and suggested that CrTX may be a potential anti-lung cancer agent and sensitizer of Iressa.

Acknowledgements

This study was supported by the National Natural Science Foundation of China (no. 81060215).

References

1. Dempke WC, Suto T and Reck M: Targeted therapies for non-small cell lung cancer. *Lung Cancer* 67: 257-274, 2010.
2. Centers for Disease Control and Prevention (CDC): Lung Cancer Fact Sheet. CDC, Atlanta, GA, USA, 156-157, 2009.
3. Rübsamen K, Breithaupt H and Habermann E: Biochemistry and pharmacology of the crotoxin complex. I. Subfractionation and recombination of the crotoxin complex. *Naunyn Schmiedeberg's Arch Pharmacol* 270: 274-288, 1971.
4. Délot E and Bon C: Model for the interaction of crotoxin, a phospholipase A2 neurotoxin, with presynaptic membranes. *Biochemistry* 32: 10708-10713, 1993.
5. Faure G, Harvey AL, Thomson E, Saliou B, Radvanyi F and Bon C: Comparison of crotoxin isoforms reveals that stability of the complex plays a major role in its pharmacological action. *Eur J Biochem* 214: 491-496, 1993.
6. Aird SD, Kaiser, II, Lewis RV and Kruggel WG: A complete amino acid sequence for the basic subunit of crotoxin. *Arch Biochem Biophys* 249: 296-300, 1986.
7. Corin RE, Viskatis LJ, Vidal JC and Etcheverry MA: Cytotoxicity of crotoxin on murine erythroleukemia cells in vitro. *Invest New Drugs* 11: 11-15, 1993.
8. Rudd CJ, Viskatis LJ, Vidal JC and Etcheverry MA: In vitro comparison of cytotoxic effects of crotoxin against three human tumors and a normal human epidermal keratinocyte cell line. *Invest New Drugs* 12: 183-184, 1994.
9. Newman RA, Vidal JC, Viskatis LJ, Johnson J and Etcheverry MA: VRCTC-310 - a novel compound of purified animal toxins separates antitumor efficacy from neurotoxicity. *Invest New Drugs* 11: 151-159, 1993.
10. Yan CH, Yang YP, Qin ZH, Gu ZL, Reid P and Liang ZQ: Autophagy is involved in cytotoxic effects of crotoxin in human breast cancer cell line MCF-7 cells. *Acta Pharmacol Sin* 28: 540-548, 2007.
11. Zhang M, Zhang X, Bai CX, Chen J and Wei MQ: Inhibition of epidermal growth factor receptor expression by RNA interference in A549 cells. *Acta Pharmacol Sin* 25: 61-67, 2004.
12. Wang JH, Xie Y, Wu JC, *et al*: Crotoxin enhances the antitumor activity of gefinitib (Iressa) in SK-MES-1 human lung squamous carcinoma cells. *Oncol Rep* 27: 1341-1347, 2012.
13. Wang Q, Tan YX, Ren YB, *et al*: Zinc finger protein ZBTB20 expression is increased in hepatocellular carcinoma and associated with poor prognosis. *BMC Cancer* 11: 271, 2011.
14. Weidner N, Semple JP, Welch WR and Folkman J: Tumor angiogenesis and metastasis - correlation in invasive breast carcinoma. *N Engl J Med* 324: 1-8, 1991.
15. Donato NJ, Martin CA, Perez M, Newman RA, Vidal JC and Etcheverry M: Regulation of epidermal growth factor receptor activity by crotoxin, a snake venom phospholipase A2 toxin. A novel growth inhibitory mechanism. *Biochem Pharmacol* 51: 1535-1543, 1996.
16. Condrea E: Membrane-active polypeptides from snake venom: cardiotoxins and haemocytotoxins. *Experientia* 30: 121-129, 1974.
17. Yan CH, Liang ZQ, Gu ZL, Yang YP, Reid P and Qin ZH: Contributions of autophagic and apoptotic mechanisms to CrTX-induced death of K562 cells. *Toxicon* 47: 521-530, 2006.
18. Cura JE, Blanzaco DP, Brisson C, *et al*: Phase I and pharmacokinetics study of crotoxin (cytotoxic PLA(2), NSC-624244) in patients with advanced cancer. *Clin Cancer Res* 8: 1033-1041, 2002.
19. Stinchcombe TE and Bogart JA: Novel approaches of chemoradiotherapy in unresectable stage IIIA and stage IIIB non-small cell lung cancer. *Oncologist* 17: 682-693, 2012.
20. Li Y and Song L: Research progress on resistance mechanisms of epidermal growth factor receptortyrosine kinase inhibitors in non-small cell lung cancer. *Zhongguo Fei Ai Za Zhi* 15: 106-111, 2012 (In Chinese).
21. Brand TM, Iida M, Li C and Wheeler DL: The nuclear epidermal growth factor receptor signaling network and its role in cancer. *Discov Med* 12: 419-432, 2011.